J Mater Sci (2008) 43:3234–3239
DOI 10.1007/s10853-008-2551-z

Dislocations in plastically deformed apatite

H. Saka · D. Goto · W.-J. Moon

Received: 22 September 2007 / Accepted: 11 February 2008 / Published online: 11 March 2008

Abstract Dislocations were introduced at room temperature by a Vickers indentation into a biological ceramic, apatite. Two types of apatite, a single crystal of fluorapatite and a sintered polycrystal of hydroxyapatite, were studied. Specimens prepared using a focused-ion-beam technique were examined by transmission electron microscopy. Natures of dislocations were determined by the conventional $\mathbf{g} \cdot \mathbf{b}$ criterion, where the weak-beam method was also applied. The slip system in fluorapatite apatite was determined to be $[0001>/(10\bar{1}0)$.

Introduction

Hydroxyapatite [HA; $Ca_5(PO_4)_3OH$] is one of the most important biomedical ceramics. HA crystallizes in hexagonal; $P6_3/m$. HA is used as a bone-grafting material because of its bioactivity. The bioactivity or the enhancement of bone–tissue formation rates and bone–tissue bonding of HA ceramics depends on its microstructure, and in particular on defects [1]. Among the defects, dislocations are shown to have an important role in in vivo dissolution and in crystal maturation [2]. Some attempts have been made to observe directly dislocations in HA by transmission electron microscopy (TEM). Nelson et al. [3] observed edge-like dislocations with Burgers vector $\mathbf{b} = \langle 0001 \rangle$ in lattice imaging micrographs. Porter et al. [4] used the conventional diffraction contrast method and showed the evidence for the presence of screw- or mixed-type dislocations in sintered HA. They claimed that the presence of dislocations is a result of sintering process and not from the mechanical process involved in specimen preparation process.

Needless to say, dislocations play a crucial role in determining mechanical properties of crystalline materials. This is the case for metals and alloys, semiconductors, minerals, and ceramics [5–7]. Among them the latter three materials are brittle at room temperatures, and the dislocations investigated by TEM were mainly introduced at high temperatures, where these materials are ductile enough to be deformed plastically by conventional tensile, compression, and bending tests. Thus, the natures of dislocations introduced at and below room temperature in most of the brittle materials remained to be studied.

One way to introduce dislocations into the brittle materials at low temperatures is by indentation, where dislocations can be introduced, albeit in a localized region underneath the image of indentation. However, to carry out TEM observation on the indented area, foil specimens with electron transparency must be prepared from the very indented region. Needless to say, preparation of TEM specimens with such site specificity is not easy with conventional specimen preparation techniques such as electro/chemical polishing and ion milling. However, recent development of focused-ion-beam (FIB) technique [8] has allowed us to prepare TEM specimens from pre-selected areas at and/or around the indented materials with at a pinpointing accuracy [9, 10].

The purpose of the present study is to study dislocations in apatite. Apatite is calcium phosphate with a chemical form of $Ca_5(PO_4)_3(OH,F,Cl)$. $Ca_5(PO_4)_3OH$ is called HA, $Ca_5(PO_4)_3F$ is called fluorapatite, and $Ca_5(PO_4)_3Cl$ is called chlorapatie. In the present study, HA and fluorapatite were studied.

H. Saka (✉) · D. Goto · W.-J. Moon
Department of Quantum Engineering, Nagoya University,
Nagoya 464-8603, Japan
e-mail: saka@nagoya-u.jp

Experimental procedures

Two types of apatite were used in the present study. One was a single crystal of fluorapatite and the other was a polycrystalline compact of HA. The latter was sintered at 1,150 °C and had a density ranging from 2.83 to 3.14 g/cm^3 (90–99% of the theoretical density). These samples of apatite were indented by a Vickers indenter with a load of 50 g at room temperature (in the case of the single crystal of fluorapatite the indented surface was (0001)). Three hundred micrometer thick slices that contained the images of indentation were sectioned with a wheel saw. These slices were thinned mechanically to 30–50 μm and transferred to a FIB milling apparatus to prepare specimens for TEM observation. The particular FIB that we used was a Hitachi FB2000 operating at an accelerating voltage of 30 kV. The TEM specimens were examined in Hitachi 9000NAR and Hitachi HU-1000D microscopes at accelerating voltages of 300 and 1,000 kV, respectively.

Results and discussion

Single crystal of fluorapatite

Figure 1 shows the crystal structure of apatite. Apatite crystallizes in hexagonal; $P6_3/m$. The crystal structure of hyroxyapatite is quite similar to that of fluorapatite.

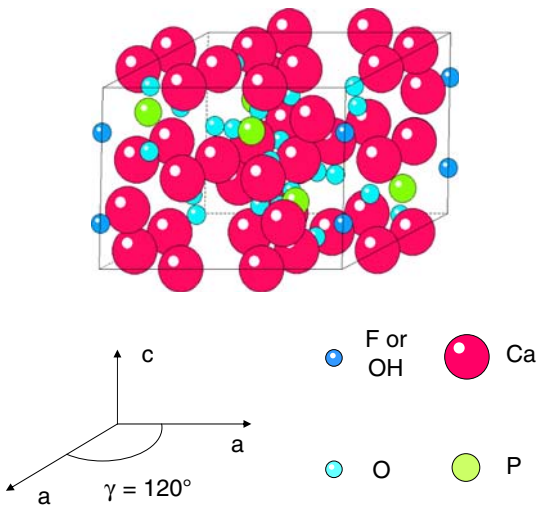

	hydroxyapatite	fluorapatite
Composition	$Ca_{10}(PO_4)_6(OH)_2$	$Ca_{10}(PO_4)_6F_2$
a (nm)	0.94282	0.93684
c (nm)	0.68777	0.68841

Fig. 1 Crystal structure of apatite. Hexagonal: $P6_3/m$

Figure 2 shows a low-magnification micrograph of the defect structure beneath an image of a Vickers indentation. The outermost black layer, denoted by W, is a protective layer of tungsten that was deposited prior to FIB thinning. Many lateral cracks are observed. In addition to the lateral cracks, a high density of lattice defects can be seen just underneath the image of the indentation. Some of the defects extended in the form of trains vertically into a deeper region, as labeled by A, B, C, D, and E.

Figure 3 shows the part indicated by A in Fig. 2 imaged under different reflection vectors at a higher magnification. It is evident that most of defects introduced by indentation are indeed dislocations. All the dislocations shown here appear strongly in $\mathbf{g} = 0002$, $\bar{1}\bar{1}21$, and $11\bar{2}1$, while they disappeared in $\mathbf{g} = 11\bar{2}0$. Therefore, the Burgers vector $\mathbf{b}$ of these dislocations must be perpendicular to $\mathbf{g} = 11\bar{2}0$. Many of the dislocations shown in Fig. 3 apparently lie in single planes. Thus, it is natural to assume that these dislocations lie in single-slip planes that are inclined to the specimen surface. The projected width of the slip plane is

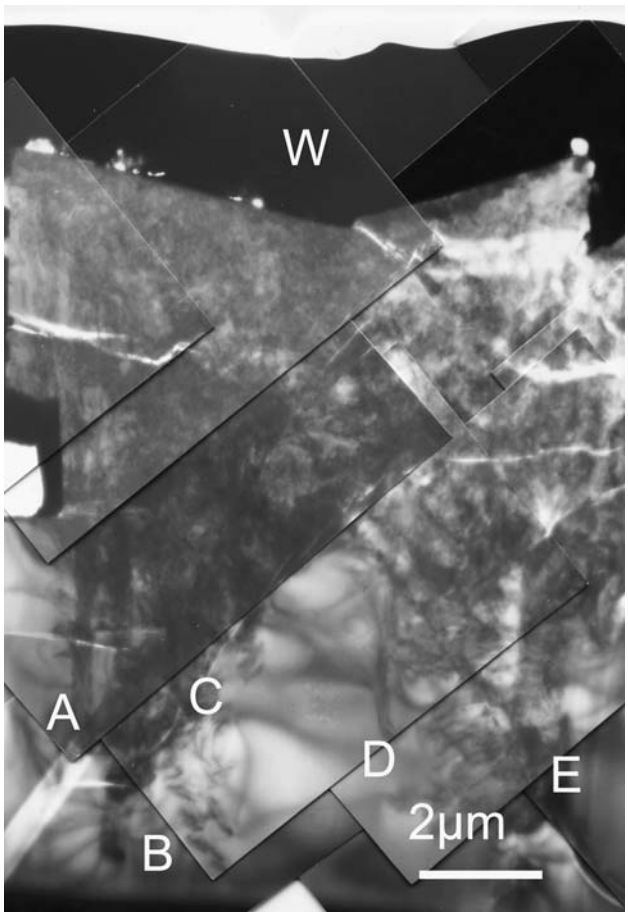

Fig. 2 Low-magnification micrograph of defect structure beneath an image of indentation performed on fluorapatite with a load of 50 g at room temperature

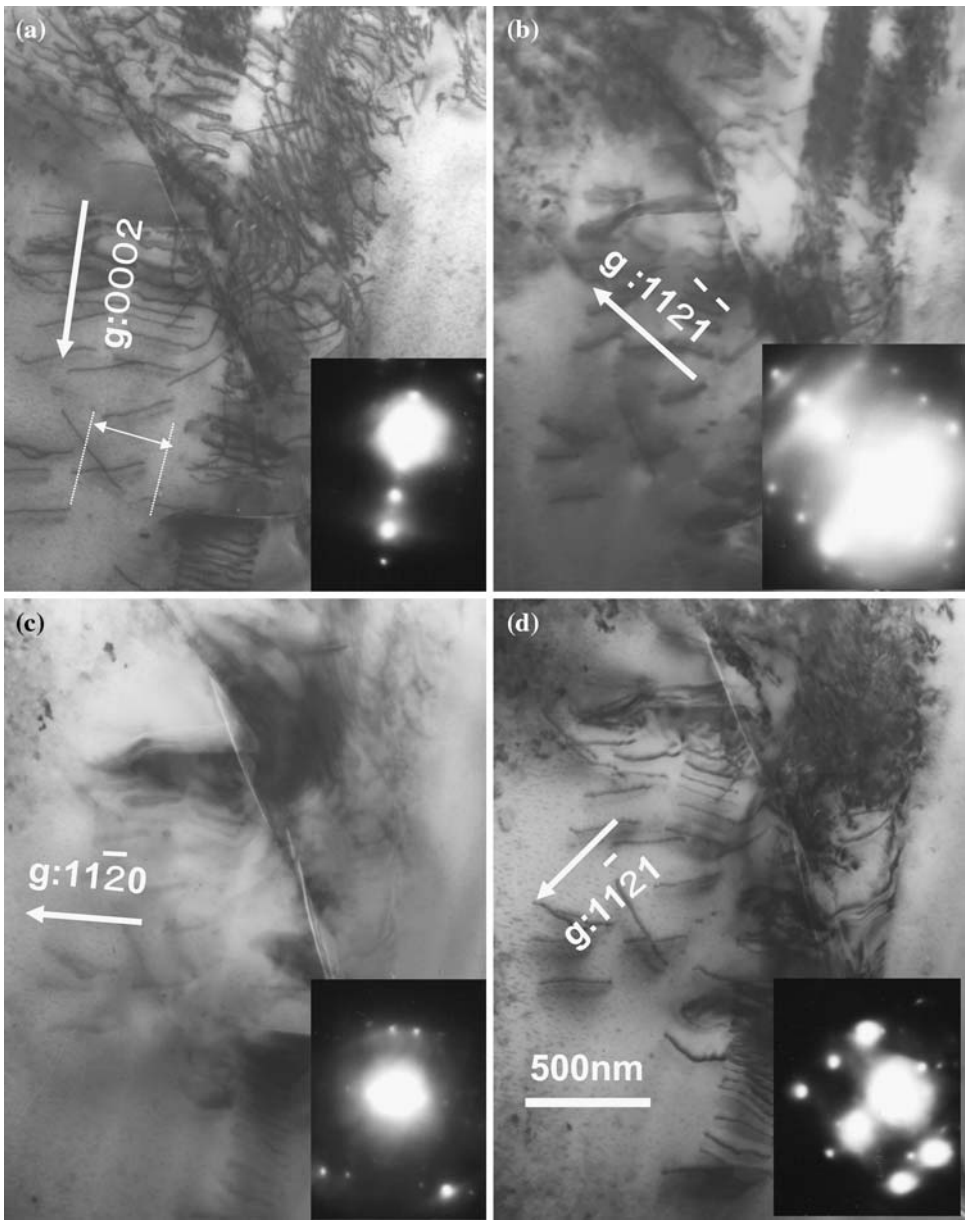

Fig. 3 Dislocations in fluorapatite imaged with different reflection vectors **g**; (**a**) 0002, (**b**) $11\bar{2}\bar{1}$, (**c**) $11\bar{2}0$, and (**d**) $11\bar{2}1$. Insets show diffraction patterns. Arrows indicate the directions of the reflection vectors excited. The dislocations disappeared in $\mathbf{g} = 11\bar{2}0$ (**c**)

about 230 nm, while the thickness of the specimen is around 450 nm, as estimated by the image during FIB thinning. This leads to the conclusion that the slip plane is inclined by $\sim 60°$ to the foil normal, as shown in Fig. 4a. Figure 4b shows the stereo projection of the normals of some crystallographic planes around $\mathbf{B} = 1\bar{1}00$ direction. It is apparent that the slip plane under consideration corresponds to $(10\bar{1}0)$ plane. Thus, the Burgers vector of these dislocations is determined to be [0001]-edge type. In other words, the slip system in fluorapatite is $[0001]/(10\bar{1}0)$.

Porter et al. [4] analyzed Burgers vector of dislocations in HA in the as-sintered state. They identified the Burgers vectors of the dislocations to be of $\langle 0001 \rangle$ screw type or $(1/3)\langle \bar{2}113 \rangle$ mixed type. This result is slightly different from that obtained in this study. Apart from the obvious difference in materials (HA versus fluorapatite), one possible explanation for the difference is that those dislocations analyzed by Porter et al. were introduced at high temperatures during sintering, while those in the present study were introduced by plastic deformation at room temperature. It is not surprising that the nature of dislocations introduced at high temperature be different from those introduced at room temperature.

Figure 5a, b shows micrographs taken under the reflection vectors of $\mathbf{g} = \bar{1}\bar{1}21$ and $\mathbf{g} = 0002$ in the weak-beam imaging mode [11]. No evidence was obtained for dissociation into partials at least within the resolution that is allowed by the weak-beam method.

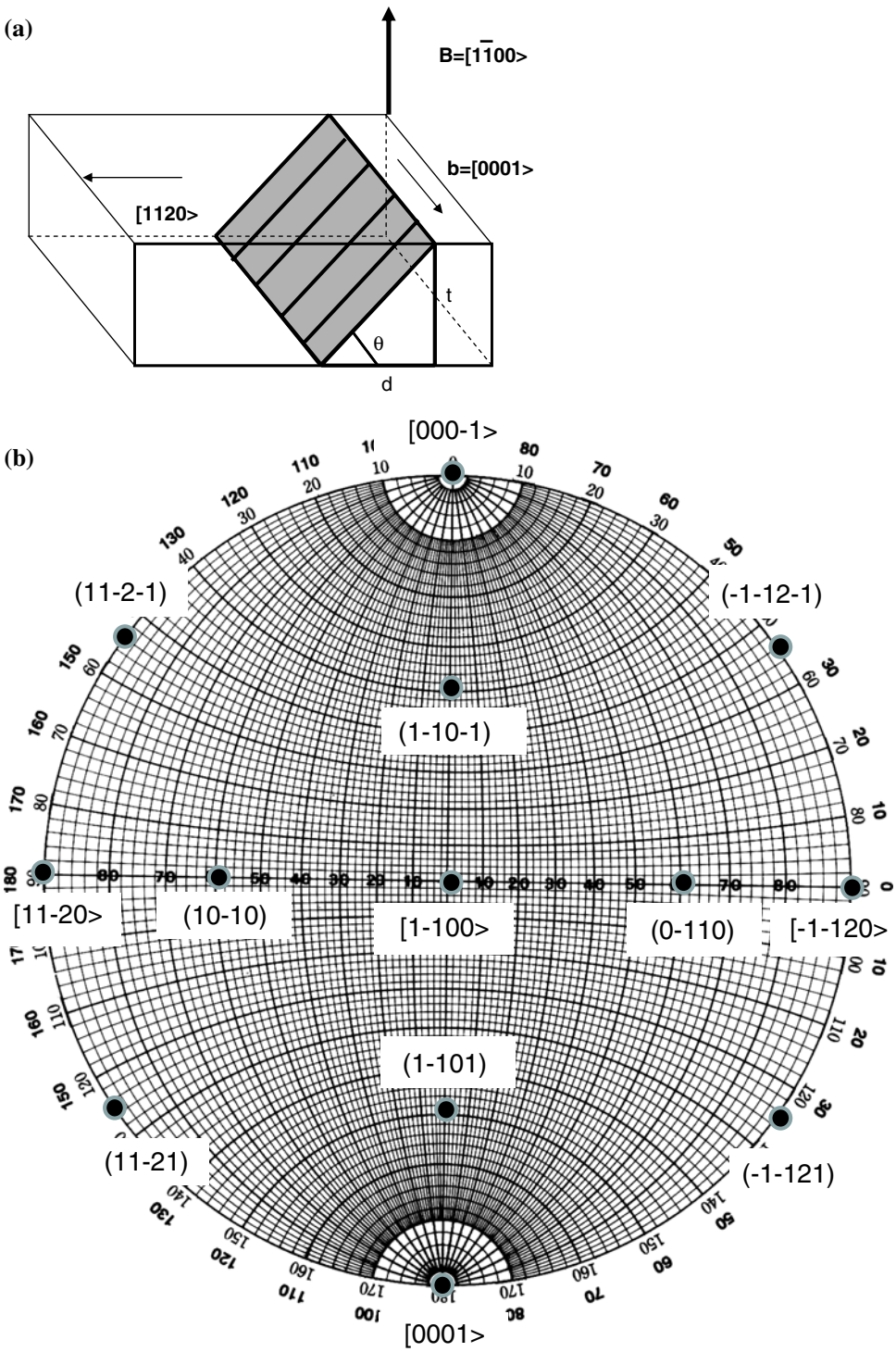

Fig. 4 (**a**) Geometry of dislocations shown in Fig. 3. (**b**) Stereo projection of the relevant crystallographic planes and orientations in apatite around [1$\bar{1}$00> direction

Sintered polycrystalline HA

Figure 6 shows a low-magnification micrograph of the defect structure beneath an image of a Vickers indentation in a polycrystalline HA. The profile of the image of indentation can be seen clearly. Two types of crack are evident: one is vertical (indicated by the white arrow) and the other is lateral (indicated by the black arrow). In addition to these cracks, there is a severely damaged region just beneath the image of indentation, as indicated by the semicircle. The damaged region extends to several micrometers from the bottom of the image of the indenter.

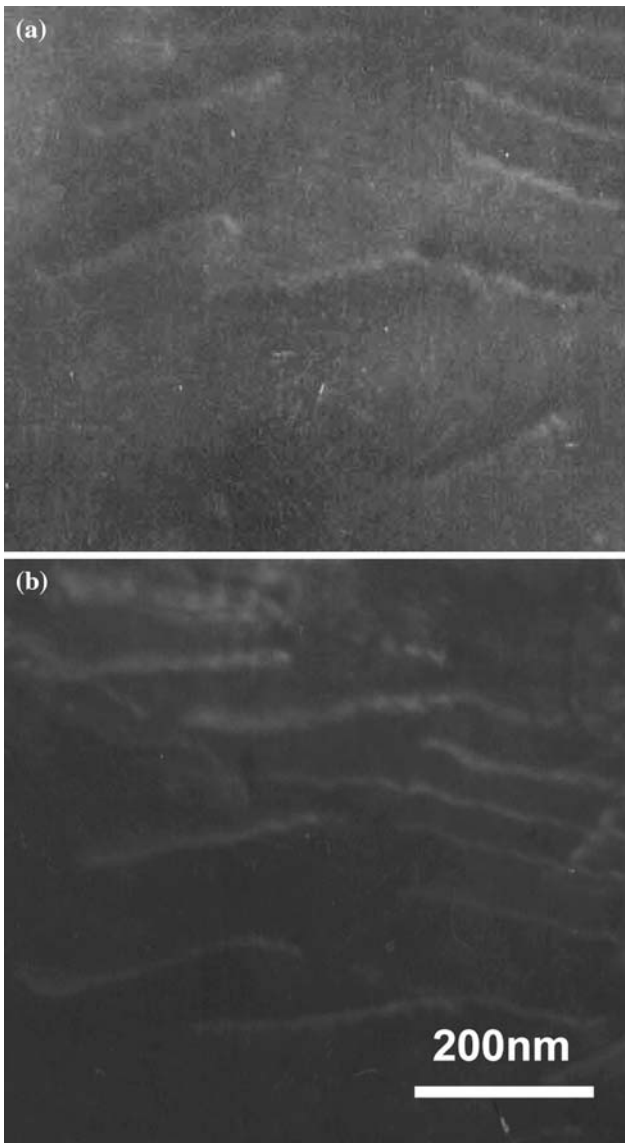

Fig. 5 Weak-beam electron micrographs of dislocations in fluorapatite imaged in $\mathbf{g} = 11\bar{2}1$ (**a**) and $\mathbf{g} = 0002$ (**b**)

Figure 7 shows a typical microstructure of the border between the severely damaged region and undamaged region. In the damaged region, complex contrasts can be seen inside grains. These contrasts must result from lattice defects themselves and also the elastic buckling of the foil caused by the defects. Outside the damaged region, however, individual grains with no apparent defects can be observed clearly. Near the border between the severely damaged and undamaged regions some grains contain moderate density of defects, which can be resolved clearly. Figure 8 shows two damaged grains, A and B, which lie

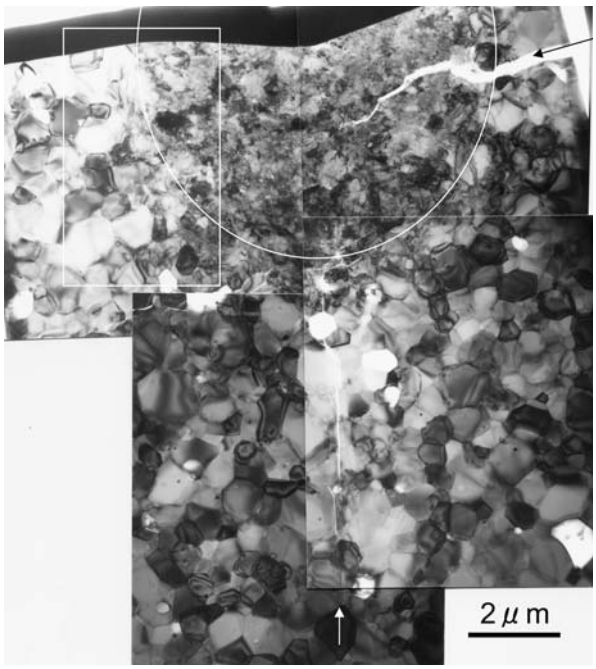

Fig. 6 Low-magnification micrograph of defect structure beneath an image of indentation performed on HA with a load of 50 g at room temperature

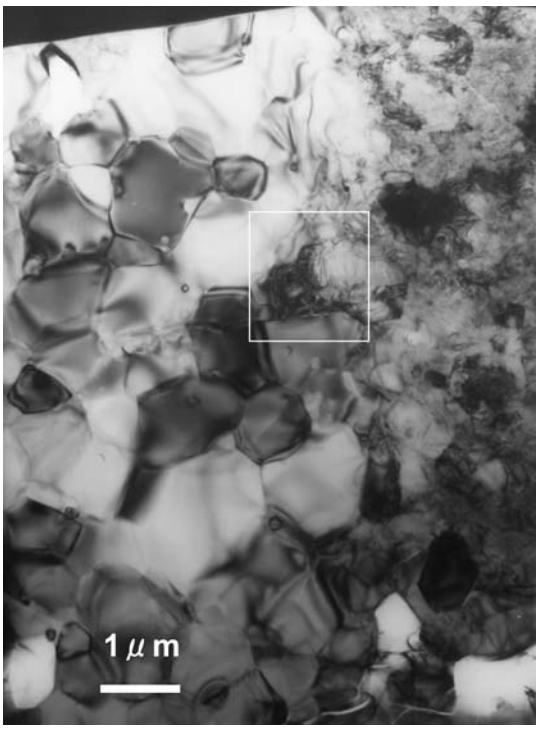

Fig. 7 Micrograph showing the boundary between the severely damaged region and undamaged region. Enlargement of the squared region in Fig. 6

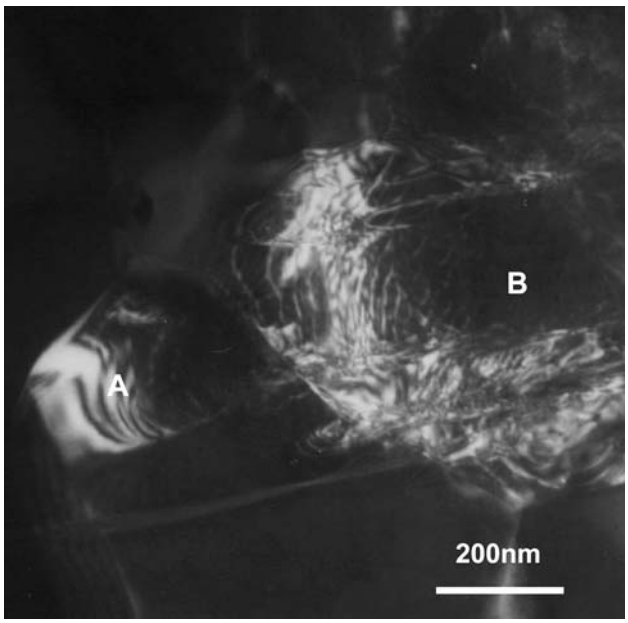

Fig. 8 Defect structures in grains A and B, just at the periphery of the damaged region. Enlargement of the squared region in Fig. 7. Dislocations are evident

just in the periphery of the damaged region, imaged in the strong dark-field mode. In grain B, which is closer to the center of the damaged region than A, many dislocations can be seen. In grain A, less density of dislocations is seen. Anyway, it is clear that dislocations are introduced by indentation at room temperature into HA.

The Burgers vector of dislocations shown in Fig. 8 could not be determined because the grain was too small for the contrast experiment to be carried out. However, judging from the similarity of the crystal structure between fluorapatite and HA, it would be reasonable to assume that the dislocations in HA have a slip system of $[0001]/(10\bar{1}0)$.

Concluding remarks

It is rather surprising that dislocations can be introduced at room temperature into apatite. This has brought out the possibility to enhance fracture toughness of apatite, which is as low as 0.7–1.2 Pa $m^{1/2}$. Moon et al. [12, 13] have shown that the fracture toughness of ceramic materials can be enhanced substantially by introducing dislocations by indentation or shot peening. This toughening technique may be applied to apatite, a very important biological ceramic.

References

1. Daculsi G, LeGeros RZ, Mitre D (1989) Calcif Tissue Int 45:95
2. Arends J, Jongebloed WL (1977) Caries Res 11:186
3. Nelson DG, McLean JD, Sanders JV (1983) J Ultrastruct Res 84:1
4. Porter AE, Best SM, Bonfield W (2004) J Biomed Mat Res A 68A:133
5. Amelincks S (1979) In: Nabarro FRN (ed) Dislocations in solids, vol 2. North-Holland Publishing Co., Amsterdam, p 67
6. (1976) In: Wenk H-R (ed) Electron microscopy in mineralogy. Springer-Verlag, Berlin, Heidelberg, New York
7. Mitchell TE, Heuer AH (2004) In: Nabarro FRN, Hirth JP (eds) Dislocations in solids, vol 12. Elsevier, p 339
8. Kirk ECG, Williams DA, Ahmed H (1988) Inst Phys Conf Ser 100:501
9. Saka H, Nagaya G (1995) Phil Mag Lett 72:251
10. Asaoka K, Umeda T, Arai S, Saka H (2005) Mater Sci Eng A 400–401:93
11. Cockayne DJH, Ray ILF, Whelan MJ (1969) Phil Mag 20:1265
12. Moon W-J, Saka H (2000) Phil Mag Lett 80:461
13. Moon W-J, Ito T, Uchimura S, Saka H (2004) Mater Sci Eng A 387–389:837